CrossMark

ORIGINAL ARTICLE

Kinetics and release characteristics of menthyl acetate from its β-cyclodextrin inclusion complex by thermogravimetric analysis

Guangyong Zhu[1] · Zuobing Xiao[1] · Rujun Zhou[1] ·
Guangxu Zhu[2] · Yuwei Niu[1]

Abstract Menthyl acetate has a characteristic, fresh, pungent flavor and a cool mouthfeel. It has been widely used in many products. Because of its high volatility and short shelf-life, menthyl acetate-β-cyclodextrin inclusion complex was produced to provide protection, enhance stability and control release of menthyl acetate. The inclusion complex was characterized by Fourier transform infrared spectroscopy, x-ray diffraction. The results show that menthyl acetate was successfully encapsulated in β-cyclodextrin. Menthyl acetate loading capacity was obtained from the weight loss difference between blank β-cyclodextrin and inclusion complex, and the value is about 8.5 %. Kinetics and release characteristics of menthyl acetate from complex were determined by thermogravimetric analysis. Menthyl acetate release mainly occurred in the first stage before β-CD decomposition. Because menthyl acetate-β-CD inclusion complex is a poor conductor of heat, the methyl acetate release peak shifted towards higher temperature with an increase in heating rate. Menthyl acetate release activation energies were obtained and the average value is 258.7 kJ/mol. Kinetics and release characteristics are basis data for better understanding the mechanism and the combination of host and guest.

Keywords Kinetics · Release · Menthyl acetate · Inclusion complex · Cyclodextrin

Introduction

Menthyl acetate (MA), as a normal constituent of peppermint oil in varying amounts depending on the source, has a fresh odor similar to mint and rose on dilution [1, 2]. It has a characteristic, fresh, pungent flavor, different from menthol (being much milder). It has a cool mouthfeel with only a trace of mint flavor. MA is a flavor ingredient and has been widely used in many products, such as pharmaceuticals, toothpastes, tobacco, chewing gum, cosmetics, and confectionery [3]. However, MA has high volatility and its shelf-life is not long. Encapsulation technology can provide protection, prevent the loss, improve shelf-life and enhance the stability of the entrapped ingredient [4]. β-cyclodextrin (β-CD) possesses a special ability to complex volatile or unstable hydrophobic compounds because its molecule has a hydrophilic outside and an apolar cavity. β-CD has been used extensively for stabilization, masking or controlled release of hydrophobic substances [5–9].

Thermogravimetric analysis (TGA) is a method of thermal analysis, which can provide information about physical and chemical phenomena including vaporization, sublimation, adsorption, desorption, chemisorptions, desolvation, and decomposition [10, 11]. The most important thing is to study degradation mechanisms and reaction kinetics with TGA. It can present information about activation energy, which can be used to evaluate the combination of guest and host. In this paper, MA-β-CD inclusion complex was produced and characterized by Fourier transform infrared (FTIR) spectroscopy, X-ray diffraction (XRD). The MA release characteristics from the MA-β-CD inclusion complexes and release activation energies were determined using thermogravimetric (TG) analysis. These are basis data for understanding the mechanism and the combination of host and guest.

✉ Zuobing Xiao
  zbingxiao@sina.com

[1] Shanghai Institute of Technology, Shanghai 201418, People's Republic of China

[2] 14846, 43Ave., Edmonton, AB T6H 5S1, Canada

Springer

Materials and methods

Materials

Menthyl acetate (MA) was provided by the Peking University Zoteq Co. Ltd. β-CD (white crystalline powder, pharmaceutical grade) and anhydrous ethanol were purchased from Sinopharm Chemical Reagent Co. Ltd (Shanghai, China). Deionized water was used throughout the experiments. All reagents were used without further purification.

Preparation of MA-β-CD inclusion complex

The method of preparation of MA-β-CD inclusion complex was adopted as described in literatures [10–12]. 3 g of β-CD was dissolved in 100 g of deionized water. The temperature was kept at 35° Con a hot plate. Then 2 g MA was slowly added to the warm β-CD solution. The mixture was continuously stirred for another 3 h and the temperature maintained at 35 °C to form MA-β-CD inclusion complex. When its temperature decreased spontaneously to room temperature, the solution was refrigerated overnight at 5 °C. The cold precipitated material was recovered by vacuum filtration. The precipitate was washed by anhydrous ethanol and dried in a FD-1C-50 freeze drier for 48 h at a temperature lower than −50 °C and pressure of around 20×10^{-3} kPa. The dried samples were washed with anhydrous ethanol and dried again. The dried MA-β-CD inclusion complex was collected and stored in a desiccator at room temperature prior to further FTIR, XRD and TG analysis.

Fourier transform infrared (FTIR) spectroscopy

FTIR spectra of MA, β-CD, MA-β-CD inclusion complex were characterized by IR spectrometry (IRAffinity-1, Shimadzu Company, Japan) in the frequency range of 4000–500 cm^{-1} with resolution of 2 cm^{-1}.

X-ray diffraction (XRD)

XRD patterns of MA, β-CD and MA-β-CD inclusion compound were investigated by an X-ray diffractometer (D/Max 2000X), Rigaku Corporation, Japan). The patterns were recorded in the region of 2θ from 5° to 70° with Cu Kα radiation at 40 kV and 100 mA.

Thermogravimetric analysis

The experiments were carried out in a TGA-Q5000IR thermogravimetric analyzer (TA Instruments, USA) to measure and record the weight loss with temperature over the course of the pyrolysis reaction. In the experiment,

approximately 5 mg of dried sample was spread uniformly on the bottom of the ceramic crucible of the thermal analyzer. The pyrolysis experiment was performed at different heating rates of 5, 10 and 20 °C/min in a dynamic high purity nitrogen flow of 20 ml/min. Nitrogen gas was used as an inert purge gas to displace air in the pyrolysis zone, thus avoiding unwanted oxidation of the sample. The temperature of the furnace was programmed to rise from room temperature to 600 °C.

Results and discussions

FTIR results of MA, β-CD and MA-β-CD inclusion complex

Figure 1 shows the FTIR spectra of β-CD, MA and MA-β-CD inclusion complex. In the curve of β-CD, there is a broad band locating at 3336 cm^{-1} which can be assigned to the stretching (O–H) vibration of hydroxyl group. The wagging (C–H) vibration appears at 1368 cm^{-1}. The band at 1339 cm^{-1} is attributed to bending (O–H) vibration. A band at 1150 cm^{-1} can be assigned to stretching (–C–O–H) vibration and a strong band at 1024 cm^{-1} can be assigned to stretching (–C–O–C) vibration respectively [11, 13–15].

In the curve of MA, the bands observed at 2922 and 2870 cm^{-1} are assigned as stretching (C–H) vibration. The stretching (C=O) vibration appears at 1736 cm^{-1}. The bands at 1456 and 1370 cm^{-1} are due to deformation (C–H) vibration. The band at 1242 cm^{-1} is assigned as the stretching of C–O [13, 14].
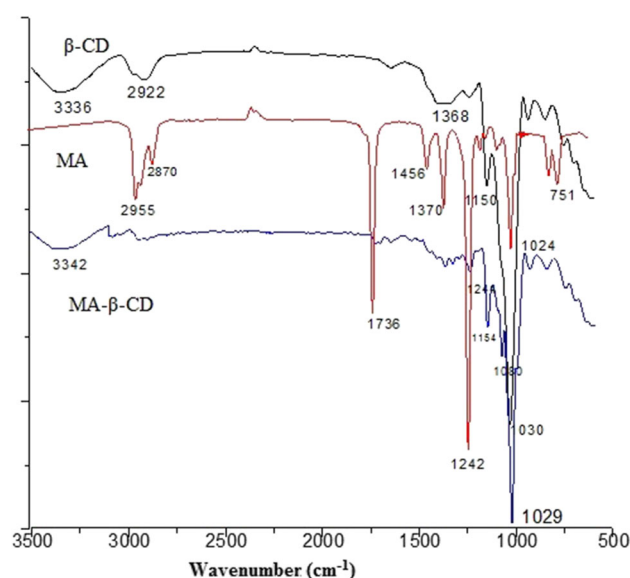

Fig. 1 FTIR spectra of β-CD, MA and MA-β-CD inclusion complex

The curve of MA-β-CD is similar to that of β-CD. This indicates that the frame of β-CD in the complex is not changed. Encapsulation of MA does not significantly change the spectra of β-CD. In the curve of MA-β-CD inclusion complex, the bands of MA at 2955, 2870, 1736, 1456, 1370, and 1242 cm^{-1} disappear or shift to other wave numbers. From these changes, it can be deduced that MA was encapsulated into the cavity of β-CD.

XRD results of β-CD and MA-β-CD inclusion complex

XRD is a useful method for the detection of CD inclusion complex. In order to see if in fact MA is encapsulated in β-CD, XRD was also used to characterize β-CD and MA-β-CD inclusion complex. The curves of XRD are shown in Fig. 2. As shown in Fig. 2, the intensity of the sharp peak at 12.7° in the XRD pattern of β-CD decreases. This peak shifts to 12.8° in the XRD pattern of MA-β-CD inclusion complex. In contrast, the peaks of 18.1°, 18.6° and 19.0° for β-CD shifted to lower 2θ angle of 16.9°, 17.2° and 17.6° for MA-β-CD inclusion complex. A similar result was also reported for the peak shift [16]. Furthermore, the peaks at 9.4°, 10.8°, 13.4° and 16.6° of β-CD disappear in the XRD pattern of MA-β-CD inclusion complex. A relatively strong peak at 11.1° appears in the XRD pattern of MA-β-CD inclusion complex. From these changes and the results of FTIR, it can be inferred that MA was encapsulated in β-CD.

Thermogravimetric characteristics

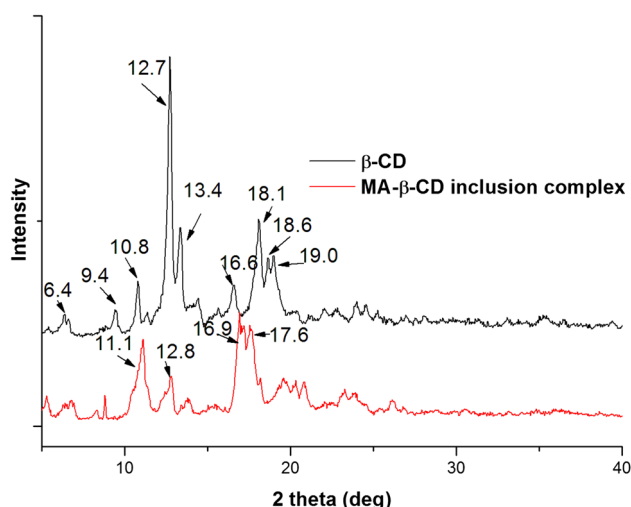Figure 3 shows the weight loss and the rate of weight loss curves obtained during the pyrolysis of MA, blank β-CD and MA-β-CD inclusion complex under inert atmosphere at a heating rate of 10 °C/min.

During thermal degradation of MA, it can be seen from the TG curve of MA as shown in Fig. 3 that MA vaporized quickly from room temperature to 120.8 °C. A strong peak appeared at 114.1 °C in the DTG curve of MA. At this peak temperature, the rate of weight loss of MA attained maximum. From 120.8 to 600 °C, the TG curve of MA was horizontal and the weight loss dropped to zero. MA vaporized almost completely before 120.8 °C.

During thermal degradation of blank β-CD, three stages can be observed during the heating process of the sample. The first stage goes from room temperature to 288.7 °C; a slight weight loss, 4.2 %, in the weight loss curve is observed. This could be due to the loss of water and light volatile compounds. The second stage goes from 288.7 to 372.7 °C. The second stage was characterized by a major weight loss, which corresponded to the main pyrolysis process of β-CD. Most of β-CD was decomposed in this stage. A strong peak appeared in the DTG curve. At the peak temperature, the rate of weight loss attained maximum. The main strong peak was due to the decomposition of β-CD. The third stage goes from 372.7 °C to the final temperature (600 °C). In the third stage, the carbonaceous matters in the solid residuals continuously decomposed at a very slow rate. A slight continued loss of weight was shown in the weight loss curve.

During thermal degradation of MA-β-CD inclusion complex, three main stages can also be distinguished during the heating process of the sample. A strong peak also appeared in the DTG curve of MA-β-CD inclusion complex due to the decomposition of β-CD. Compared to the pyrolysis characteristic of blank β-CD, although the TG curve of MA-β-CD inclusion complex is similar to that of the blank β-CD, some new pyrolysis characteristics appear
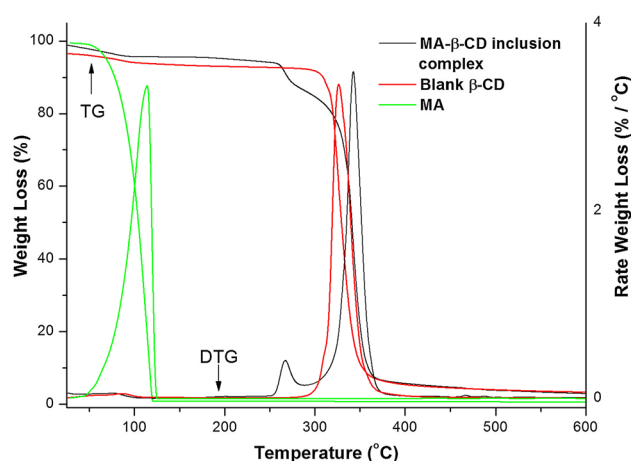

Fig. 2 XRD patterns of β-CD and MA-β-CD inclusion complex

Fig. 3 TG–DTG curves of MA, blank β-CD and MA-β-CD inclusion complex at a heating rate of 10 °C/min

especially in the first stage. The TG curve of blank β-CD shows a leveling-off from 250.1 to 288.7 °C, while the TG curve of MA-β-CD inclusion complex is downward sloping in this temperature range. In DTG curve of MA-β-CD inclusion complex, a small peak appears at 267.1 °C. It can be attributed to release of MA encapsulated in the cavities of β-CD. As shown in Fig. 3, because the small peak appears in front of decomposition peak of β-CD, MA release occurs before β-CD decomposition. The weight losses of blank β-CD and MA-β-CD inclusion complex are 4.2 and 12.7 % respectively in the first stage from room temperature to 288.7 °C. The difference, 8.5 %, of the weight losses is mainly due to MA. From the difference of the two values of weight loss, MA loading capacity can be estimated as about 8.5 %.

Compared the TG curves of MA and MA-β-CD inclusion complex, it can be seen that MA release from the MA-β-CD inclusion complex mainly occurred in the temperature range of 250.1–288.7 °C, while MA alone vaporized almost completely before 120.8 °C. Compared the DTG curves of MA and MA-β-CD inclusion complex, it can be seen that the weight loss rate of MA from MA-β-CD inclusion complex attained the maximum value at 267.1 °C, while the weight loss rate of MA alone attained the maximum value at 114.1 °C. From these data, it can be inferred that the loss of MA was prevented to some extent by encapsulation of MA in β-CD. Furthermore, the sensory character of MA and MA-β-CD inclusion complex was smelled by nose. The odor of MA alone cannot be detected after 5 days; while MA-β-CD still has characteristic odor of MA after 2 month. These results indicated that the shelf-life of MA was improved by encapsulation of MA in β-CD.

Effect of heating rate on MA release

MA release mainly occurred in the first stage, especially around the small peak temperature in the range of 250.1 to 288.7 °C as shown in Fig. 3. Therefore, the effect of heating rate on MA release was investigated in the first stage around small peak.

Figure 4 shows the weight loss and the rate of weight loss curves obtained from the pyrolysis of MA-β-CD at different heating rates (5, 10 and 20 °C/min). All the DTG curves contained small peaks, which were attributed to release of MA. At the peak temperature, the release rate of MA attained maximum. The peak shifted towards higher temperature with an increase in heating rate. This is typical for all non-isothermal experiments [17]. The main reason for these shifts may be that MA-β-CD inclusion complex is a poor conductor of heat. There exists a temperature gradient throughout the cross-section of MA-β-CD inclusion complex. At lower heating rate, the temperature profile along the cross-section can be assumed linear as both the outer surface
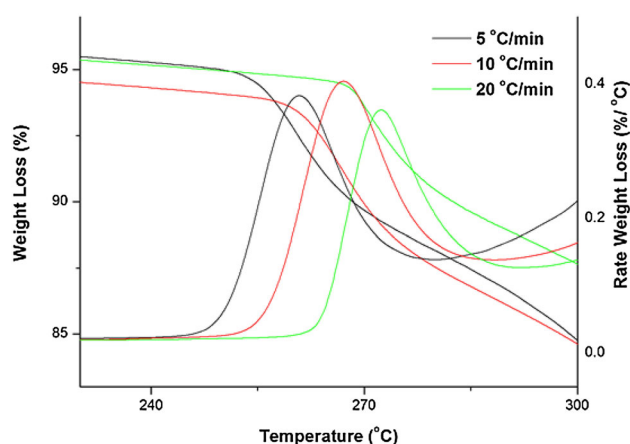

Fig. 4 TG-DTG curves of MA-β-CD inclusion complex in different heating rate against temperature

and the inner core of MA-β-CD inclusion complex attains same temperature at a particular time as sufficient time is given for heating. On the other hand, at a higher heating rate, a substantial difference in temperature profile exists along the cross-section of the MA-β-CD inclusion complex.

The analysis of the rate of weight loss curve shows that only one peak was observed during the pyrolysis process of MA-β-CD inclusion complex in the first stage. This peak was due to the release of MA. The release characteristics of MA-β-CD inclusion complex were given in Table 1.

Pyrolysis kinetic parameter of MA-β-CD inclusion complex

The analysis of TGA graphs was used to determine the kinetic parameter of MA-β-CD inclusion complex. Kissinger–Akahira–Sunose (KAS) method [18, 19], was adopted to determine activation energy from the thermogravimetric data.

In the non-isothermal experiments carried out with a thermo balance, the sample mass was measured as a function of temperature. The rate of conversion, $d\alpha/dt$, is a linear function of a temperature-dependent rate constant, k, and a function of conversion, $f(\alpha)$. The degree of conversion is expressed as Eq. (1) [10, 17].

$$\frac{d\alpha}{dt} = kf(\alpha), \tag{1}$$

Table 1 MA release characteristics at different heating rates

Heating rate (°C/min)	Peak temperature (°C)	Rate weight loss (%/°C)
5	260.9	0.3825
10	267.1	0.4039
20	272.3	0.3616

where α is the converted degree of pyrolysis reaction and $\alpha = (m_p - m_a)/(m_p - m_k)$, m_p the sample initial mass, m_a the sample mass at time t, m_k the mass at the end of the experiment, t is the time, and k is the rate constant.

In Arrhenius equation, k is also defined as:

$$k = A \exp\left(-\frac{E}{RT}\right), \tag{2}$$

where A is the pre-exponential factor, E is the activation energy, R is the gas constant, and T is the absolute temperature.

For a linear heating rate of, say, β (Kelvin/min):

$$\beta = dT/dt \tag{3}$$

The reaction rate can be expressed as Eq. (4) according to Eqs. (1)–(3).

$$\frac{d\alpha}{f(\alpha)} = \frac{A}{\beta} \exp\left(-\frac{E}{RT}\right) dT \tag{4}$$

Essentially the technique assumes that the A, $f(\alpha)$ and E are independent of T, while A and E are independent of α. The integrated form of Eq. (4) is generally written as Eq. (5).

$$G(\alpha) = \int_0^{\alpha} \frac{d\alpha}{f(\alpha)} = \frac{A}{\beta} \int_{T_0}^{T} \exp\left(-\frac{E}{RT}\right) dT = \frac{AE}{\beta R} P\left(\frac{E}{RT}\right), \tag{5}$$

where $G(\alpha)$ is the integrated form of the conversion dependence function $f(\alpha)$.

The logarithmic form of Eq. (5) is expressed as Eq. (6).

$$\ln G(\alpha) = \ln\left(\frac{AE}{R}\right) - \ln \beta + \ln P\left(\frac{E}{RT}\right), \tag{6}$$

There exists an approximation [20, 21] as Eq. (7).

$$P\left(\frac{E}{RT}\right) \approx \frac{\exp(-E/RT)}{(E/RT)^2} \tag{7}$$

From Eqs. (6) and (7), it follows that:

$$\ln \frac{\beta}{T^2} = \ln \frac{AR}{EG(\alpha)} - \frac{E}{RT} \tag{8}$$

Thus, the plot $\ln(\beta/T^2)$ versus $1/T$ for a constant value of α should result in a straight line and the slope of the line can be used to evaluate the activation energy.

The straight lines plotted are shown in Fig. 5. The activation energies obtained from the slope are summarized in Table 2. From Table 2, the activation energy values have been found in the range of 231.3–273.5 kJ/mol at various conversions α.

The interaction between MA and β-CD, and the combination of the guest and the host are important for understanding the inclusion complex process. The activation
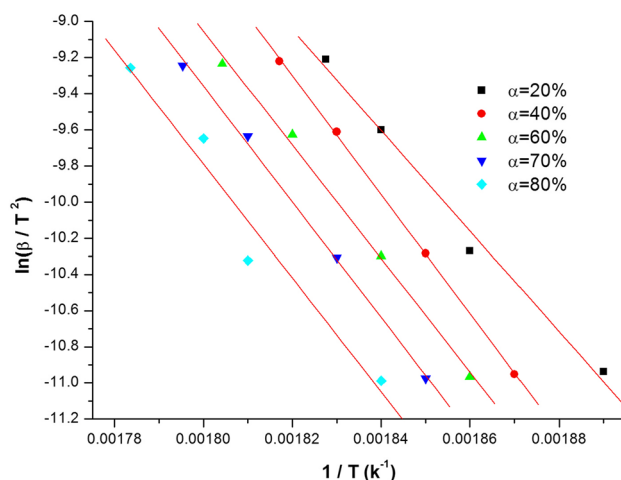

Fig. 5 Plots for determination of activation energy at different α by KAS method

Table 2 The apparent activation energies obtained by KAS method

Conversion degree (α%)	E (kJ/mol)	Correlation coefficient
20	231.3	−0.9950
40	273.5	−0.9998
60	261.3	−0.9982
70	265.8	−0.9990
80	261.8	−0.9794
Average	258.7	

energy means that energy is required to disassemble a whole MA-β-CD inclusion complex into separate parts. On the contrary, when MA enters into the cavity of β-CD, energy will be released and stable inclusion complex will be formed. From activation energy, we can infer the combination of MA and β-CD. A low activation energy means a fast reaction and a high activation energy means a slow reaction [22]. The smaller the apparent activation energy is, the more easily the reaction carries out [12]. Small activation energy indicates that MA easily release from the inclusion complex, while high activation energy implies that MA are slowly released from the MA-β-CD inclusion complex.

Conclusions

This paper deals with the production and characterization of MA-β-CD inclusion complex. The inclusion complex was successfully produced. The results of FTIR and XRD confirm that MA enters the cavity of β-CD. The MA loading capacity was determined by TG analysis, and the value is about 8.5 %. During thermal degradation of MA-β-CD inclusion complex, the first stage goes from room

temperature to 288.7 °C at a heating rate of 10 °C/min. MA release from the inclusion complex mainly occurred in the first stage before β-CD decomposition, especially around the small peak temperature in the range of 250.1–88.7 °C. The MA release peak shifted towards higher temperature with an increase in heating rate. The release peak temperatures are 260.9, 267.1 and 272.3 °C at the heating rate of 5, 10 and 20 °C/min respectively. The activation energy values were determined by KAS method. Activation energies are in the range of 231.3-273.5 kJ/mol at various conversions α, and the average value is 258.7 kJ/mol.

References

1. Burdock, G.A.: Fenaroli's Handbook of Flavor Ingredients. CRC Press, Boca Raton (2010)
2. Riachi, L.G., De Maria, C.A.B.: Peppermint antioxidants revisited. Food Chem. **176**, 72–81 (2015)
3. Geiss, O., Bianchi, I., Barahona, F., Barrero-Moreno, J.: Characterisation of mainstream and passive vapours emitted by selected electronic cigarettes. Int. J. Hyg. Environ. Health **218**, 169–180 (2015)
4. Zhu, G., Xiao, Z., Zhou, R., Yi, F.: Fragrance and flavor microencapsulation tech-nology. Adv. Mater. Res. **535–537**, 440–445 (2012)
5. Fernandes, A., Ivanova, G., Brás, N.F., Mateus, N., Ramos, M.J., Rangel, M., de Freitas, V.: Structural characterization of inclusion complexes between cyanidin-3-O-glucoside and β–cyclodextrin. Carbohydr. Polym. **102**, 269–277 (2014)
6. Gomes, L.M.M., Petito, N., Costa, V.G., Falcão, D.Q., de Araújo, K.G.L.: Inclusion complexes of red bell pepper pigments with β-cyclodextrin: preparation, characterisation and application as natural colorant in Yogurt. Food Chem. **148**, 428–436 (2014)
7. Santos, E.H., Kamimura, J.A., Hill, L.E., Gomes, C.L.: Characterization of carvacrol beta-cyclodextrin inclusion complexes as delivery systems for antibacterial and antioxidant applications. LWT Food Sci. Technol. **60**, 583–592 (2015)
8. Szwajca, A., Koroniak, H.: Encapsulation of fluoroaromatics by β-cyclodextrin and their derivatives theoretical studies. J. Fluorine Chem. **167**, 122–127 (2014)
9. Zeng, Z., Fang, Y., Ji, H.: Side chain influencing the interaction between β-cyclodextrin and vanillin. Flavour Fragr. J. **27**, 378–385 (2012)
10. Zhu, G., Xiao, Z., Zhou, R., Zhu, Y.: Study of production and pyrolysis characteristics of sweet orange flavor-β-cyclodextrin inclusion complex. Carbohydr. Polym. **105**, 75–80 (2014)
11. Zhu, G., Feng, N., Xiao, Z., Zhou, R., Niu, Y.: Production and pyrolysis characteristics of citral-monochlorotriazinyl-β-cyclodextrin inclusion complex. J. Therm. Anal. Calorim. **120**, 1811–1817 (2015)
12. Zhu, G., Xiao, Z., Zhou, R., Feng, N.: Production of a transparent lavender flavour nanocapsule aqueous solution and pyrolysis characteristics of flavour nanocapsule. J. Food Sci. Technol. **52**, 4607–4612 (2015)
13. Chen, Q., Guo, P.: Inclusion compound of menthol with hydroxypropyl-β-cyclodextrin by infrared spectroscopy. Cent. South Pharm. **7**, 749–752 (2009) (**in Chinese**)
14. Fan, K.: An Introduction to Spectroscopy. Higher Education Press, Beijing (2011) (**in Chinese**)
15. Ahmed, A., Wang, H., Yu, H., Zhou, Z., Ding, Y., Hu, Y.: Surface engineered cyclodextrin embedded polymeric nanoparticles through host–guest interaction used for drug delivery. Chem. Eng. Sci. **125**, 121–128 (2015)
16. Yang, Z., Xiao, Z., Ji, H.: Solid inclusion complex of terpinen-4-ol/β-cyclodextrin: kinetic release, mechanism and its antibacterial activity. Flavour Fragr. J. **30**, 179–187 (2015)
17. Zhu, G., Zhu, X., Xiao, Z., Zhou, R., Yi, F.: Pyrolysis characteristics of bean dregs and in situ visualization of pyrolysis transformation. Waste Manag. **32**, 2287–2293 (2012)
18. Hu, R., Shi, Q.: Thermal Analysis Kinetics. Science Press, Beijing (2001) (**in Chinese**)
19. Kissinger, H.E.: Reaction kinetics in differential thermal analysis. Anal. Chem. **29**, 1702–1706 (1957)
20. Aboulkas, A., Ei Harfi, K., Ei Bouadili, A.: Thermal degradation behaviors of polyethylene and polypropylene. Part I: pyrolysis kinetics and mechanisms. Energy Convers. Manag. **51**, 1363–1369 (2010)
21. Coats, A.W., Redfern, J.P.: Kinetic parameters from thermogravimetric data. Nature **201**, 68–69 (1964)
22. Levine, I.N.: Physical Chemistry. Tsinghua University Press Limited, Beijing (2012)